

**Far-infrared measurement of the dopant-dependent residual absorptivity of  $\text{Bi}_2\text{Sr}_2\text{CaCu}_2\text{O}_{8+\delta}$** 

R. G. Buckley

*Industrial Research Limited, PO Box 31310, Lower Hutt, New Zealand*

H. S. Barowski\* and K. F. Renk

*Institut für Angewandte Physik, Universität Regensburg, D-93040 Regensburg, Germany*

(Received 28 November 2000; published 12 June 2001)

Measurements are reported of the low-frequency absorptivity of  $\text{Bi}_2\text{Sr}_2\text{CaCu}_2\text{O}_{8+\delta}$  crystals at 16 K from under to overdoping (oxygen content). At optimal doping the magnitude of the absorptivity is 0.4% between 0.6 and 7 THz and the conductivity is dominated by peaks at zero frequency and 30 THz separated by a deep minimum. The minimum is not evident in the under and overdoped samples. The increased absorptivity when doped away from optimal indicates that the spectral distribution of quasiparticles is dopant dependent due to changes in the elastic and inelastic scattering contributions.

DOI: 10.1103/PhysRevB.64.014509

PACS number(s): 74.25.Gz, 74.62.Dh, 74.72.Hs

Experimental investigations indicate that the superconducting critical temperature,  $T_c$ , of the cuprate superconductors varies with concentration of holes on the  $\text{CuO}_2$  planes.<sup>1</sup> At zero doping these materials are antiferromagnetic insulators but with increasing hole concentration they become electronically conducting and at low temperature superconducting. With further increases in hole concentration  $T_c$  first rises (underdoped region) to a maximum (optimally doped) before falling (overdoped). A key to understanding this behavior is the development of a description of the low-energy carrier dynamics as a function of electronic doping, particularly at temperatures well below  $T_c$ .

Using reflection spectroscopy the low-frequency temperature-dependent dynamical conductivity has been determined for under and overdoped cuprates including  $\text{Bi}_2\text{Sr}_2\text{CaCu}_2\text{O}_{8+\delta}$ .<sup>2</sup> It is observed that with decreasing temperature the Drude-like conductivity peak centered at zero-frequency strengthens and narrows. As the temperature approaches  $T_c$  the behavior becomes complex and is dopant dependent. At optimal doping a “gap-like” feature appears in the conductivity spectrum at  $T_c$ . For underdoped samples the gap-feature appears above  $T_c$  and for samples that are increasingly overdoped the formation of a gap is less readily identified. Recent measurements suggest that at temperatures well below  $T_c$  a zero-frequency conductivity peak persists, although the very small absorptivity ( $\leq 1\%$ ) makes these experiments demanding using reflection spectroscopy alone. Other techniques have been applied to  $\text{YBa}_2\text{Cu}_3\text{O}_{7-\delta}$  and  $\text{Bi}_2\text{Sr}_2\text{CaCu}_2\text{O}_{8+\delta}$  thin films indicating that a zero-frequency peak does exist for optimally doped samples although little work has been done at other dopings.<sup>3</sup> Theoretical studies suggest that this peak arises from elastic scattering processes and at higher frequencies the absorption is dominated by inelastic scattering.<sup>4,5</sup> Very few measurements have been reported that probe the cross-over spectral region and so investigate the relative contributions of elastic and inelastic scattering processes to the low frequency conductivity of the cuprates.

Here we report the first measurements of the low temperature (16 K) dopant-dependent absorptivity of high quality crystals of  $\text{Bi}_2\text{Sr}_2\text{CaCu}_2\text{O}_{8+\delta}$  in a spectral region dominated

by the cross over between elastic and inelastic scattering processes. These measurements are made to a high photometric accuracy using a photothermal interference technique at low frequency (0.6 and 4 THz) coupled with reflection spectroscopy at higher frequency (6 and 1200 THz). Photothermal spectroscopy and reflectivity measurements were made to an uncertainty in the absolute absorptivity of 0.1% and  $\pm 1\%$ , respectively. We observed for an optimally doped sample that the absorptivity is approximately independent of frequency between 1 and 7 THz (4 and 30 meV) and is approximately 0.4% in magnitude over this spectral range. The high accuracy of the data allows for the determination of the dynamical conductivity down to 0.6 THz and demonstrates that the real part of the conductivity is dominated by a zero frequency peak and a peak near 30 THz separated by a deep minimum near 12 THz. In sharp contrast under and overdoped crystals have a considerably higher absorptivity between 0.6 to 9 THz. The increased absorption results from an increase in quasiparticle density when doping away from optimal which may be due to either an increase in the effectiveness of elastic scattering around nodes in the density of states and/or a change in the electron-boson spectral density function determining inelastic scattering.

$\text{Bi}_2\text{Sr}_2\text{CaCu}_2\text{O}_{8+\delta}$  crystals were grown by a floating-zone technique and a number of crystals were cleaved from the same boule.<sup>6</sup> Optical measurements were made on crystals that were typically about  $4 \times 5 \times 0.1 \text{ mm}^3$  in size, were flat and displayed a mirrorlike surface when viewed in visible light. Pairs of crystals were treated with different thermal processes to establish the required oxygen content and thus dopant level.  $T_c$ 's were determined by measuring the temperature-dependent magnetization and defined as the onset temperature, being 71 K (underdoped), 91 K (optimally doped), and 73 K (overdoped).

Photothermal interference spectroscopy involves the focusing of a modulated far-infrared laser beam on to the sample. Absorption by the sample results in a local modulated increase in temperature leading by heat diffusion, to a modulated increase in temperature of the surrounding helium gas. The oscillating change in gas temperature and the accompanying change in its refractive index is monitored with

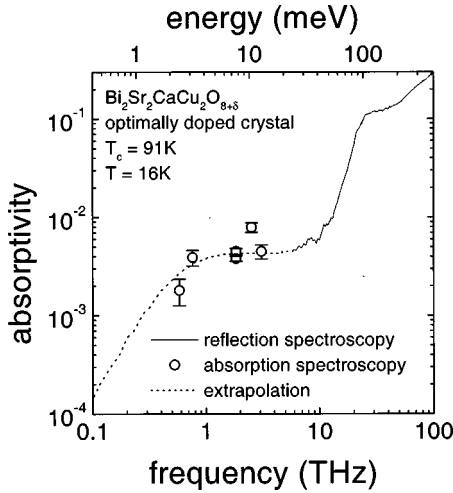


FIG. 1. The 16 K absorptivity of an optimally doped  $\text{Bi}_2\text{Sr}_2\text{CaCu}_2\text{O}_{8+\delta}$  crystal ( $T_c = 91$  K) measured using photothermal interference (circles) and reflectance spectroscopies (solid curve). The dashed curve is the extrapolation used in the Kramer-Kronig transformation.

a two-beam visible-light interferometer with one beam, the probe beam, passing near to the heated surface and a second, the reference beam, passing in a region unaffected by the modulated heating. The phase shift between these two beams, which is determined by their recombination, contains a signal proportional to the absorptivity. The magnitude was calibrated by replacing the sample with a piece of carbon of known absorptivity.<sup>7</sup>

Below we focus on the spectral region below 100 THz and first discuss the optimally doped  $\text{Bi}_2\text{Sr}_2\text{CaCu}_2\text{O}_{8+\delta}$  crystal. The 16 K absorptivity is small, approximately 0.4%, and frequency independent from 1 to 7 THz (Fig. 1). At higher frequencies the absorptivity rises across the infrared to reach very high values in the visible. The error bars represent the reproducibility of the absorptivity measurements. A Kramers-Kronig transformation was used to obtain the dynamic conductivity [ $\sigma(\omega) = \sigma_1(\omega) + i\sigma_2(\omega)$ ]. The absorptivity data were extrapolated from 1200 to 10 000 THz using the data of Terasaki *et al.*<sup>8</sup> and at higher frequencies a  $\omega^{-4}$  extrapolation was employed. Below 0.6 THz a two-fluid model was used to extrapolate the data to match the microwave absorptivity measured by Lee *et al.*<sup>9</sup> on an optimally-doped ( $T_c \approx 93$  K) floating-zone grown crystal obtained from a different source (dashed line, Fig. 1).

The real part of the conductivity,  $\sigma_1$ , is dominated by peaks centered at zero frequency and near 30 THz (Fig. 2). The conductivity falls to very low values between these peaks forming a deep minimum near 12 THz. The primary uncertainty in determining the magnitude of the zero-frequency peak is the frequency dependence of the low frequency extrapolation while the width and thus the position of the minimum are determined by the measured data above 0.6 THz. We estimate that the magnitude of the peak at zero frequency is accurate to a factor of 2. Our ability to extend spectral measurements into a region where the absorptivity is less than 1% has allowed for a clear identification of the zero frequency peak in  $\sigma_1$  for optimally doped

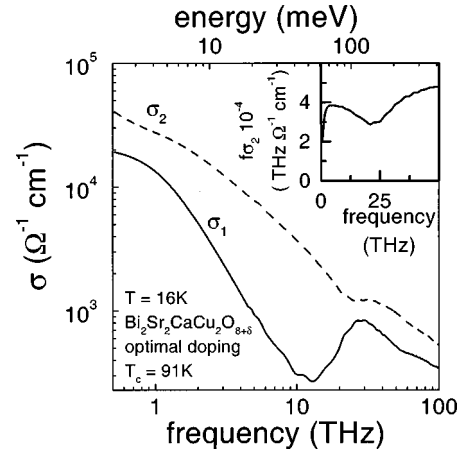


FIG. 2. The real and imaginary parts of the dynamical conductivity for optimally doped  $\text{Bi}_2\text{Sr}_2\text{CaCu}_2\text{O}_{8+\delta}$  ( $T_c = 91$  K) at 16 K. Inset: The product  $f\sigma_2$  against frequency for the same crystal where  $f$  is the frequency.

$\text{Bi}_2\text{Sr}_2\text{CaCu}_2\text{O}_{8+\delta}$ . The imaginary part of the conductivity,  $\sigma_2$ , increases with decreasing frequency consistent with the presence of both the zero-frequency peak in  $\sigma_1$  and the superconducting condensate.

Although a detailed interpretation of the conductivity spectra is not possible our results display features that are qualitatively similar to those observed in conductivity calculations for a  $d$ -wave superconductor that include inelastic and elastic scattering.<sup>4,5</sup> Notably, the presence of a zero frequency peak determined by elastic (impurity) scattering at nodes in the density-of-states by quasiparticles that do not participate in the superconducting condensate and a second peak at higher frequencies (30 THz) determined by inelastic scattering. The two features are separated by a conductivity minimum with a depth that depends on the strength of the scattering and the cross over between elastic and inelastic scattering determines its position.<sup>5</sup> The implication of the close correspondence between the calculations and the present data is that at low temperature the real part of the low frequency ( $< 10$  THz) response of optimally doped  $\text{Bi}_2\text{Sr}_2\text{CaCu}_2\text{O}_{8+\delta}$  is dominated by elastic scattering in the strong limit.<sup>4,5</sup> This conclusion is strengthened by the frequency dependence of the product,  $\omega\sigma_2$ , from which the penetration depth is often extracted ( $\lambda_L^2 = 1/\mu_0\omega\sigma_2$ ). Because of both the zero-frequency peak in  $\sigma_1$  and the condensate the behavior of  $\omega\sigma_2$  deviates considerably from the simple frequency-independent behavior often assumed, and is similar to that observed in the results of recent calculations for a  $d$ -wave superconductor (Fig. 2, inset, and Ref. 5).

We now discuss the absorptivity spectra for the under and overdoped samples (Fig. 3). These spectra contrast sharply with the spectrum of the optimally doped sample. The absorptivities of both samples in the 1 to 30 THz spectral range are significantly greater than that observed for the optimally doped sample and do not display a plateau between 1 and 7 THz. The absorptivity of the underdoped sample lies between that of the optimally and overdoped samples. At higher frequencies ( $> 30$  THz) there are only small differences among the samples. The dynamical conductivity was

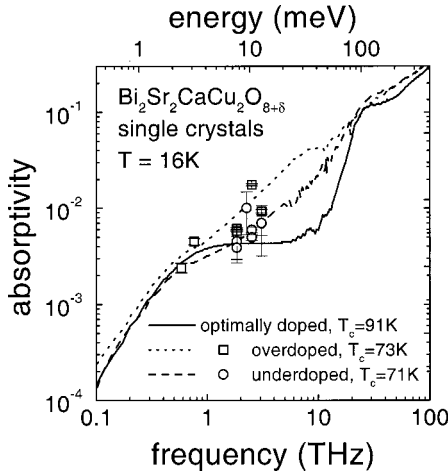


FIG. 3. Absorptivity at 16 K for under (circles and dashed curve,  $T_c = 71$  K) and overdoped crystals (squares and dotted curve,  $T_c = 73$  K) compared with the optimally doped crystal (solid curve). Below 8 THz an extrapolation was constructed for the purpose of the Kramers-Kronig analysis on the basis of the points measured using photothermal interference spectroscopy as discussed in the text.

calculated by undertaking a Kramers-Kronig analysis although a reliable low frequency extrapolation becomes more difficult to define due to the lack of measurements at microwave frequencies. The data displayed employed the same slope as that used for the optimally doped sample and was scaled to higher absorptivities by an amount equal to the difference at 1 THz between the over and optimally doped samples. The uncertainty in the resulting low frequency conductivity is a factor of 2.

$\sigma_1$  for the under and overdoped samples is characterized by higher absorption over the region of the absorption minimum in the optimally doped crystal (Fig. 4). The magnitude of the zero-frequency peak depends on the slope of the extrapolation and is thus uncertain although the increase in absorption at higher frequencies is constrained by the reliable experimental data above 1 THz. A decrease in the magnitude of  $\sigma_2$  below 20 THz with doping away from optimal is consistent with the decrease in the zero-frequency peak and/or loss of condensate. Given the uncertainties in the magnitude of  $\sigma_1$  it is not easy to separate these two contributions. The data nonetheless clearly indicates an increase in the absorption in the region of the minimum and that this increased spectral weight must be at the expense of either the condensate or it indicates there is a dopant-dependent change in the contributions of the elastic and inelastic scattering processes.

Our ability to measure the very small absorptivity at 16 K of  $\text{Bi}_2\text{Sr}_2\text{CaCu}_2\text{O}_{8+\delta}$  has allowed us to determine the low-frequency conductivity in the superconducting state as a function of oxygen content (electronic doping). We have demonstrated that the absorptivity minimum between the zero-frequency peak and the inelastic peak has been lost with doping away from optimal. These changes can arise from changes in elastic and inelastic scattering.<sup>4,5</sup> Calculations of the conductivity for  $d$ -wave superconductors conclude that

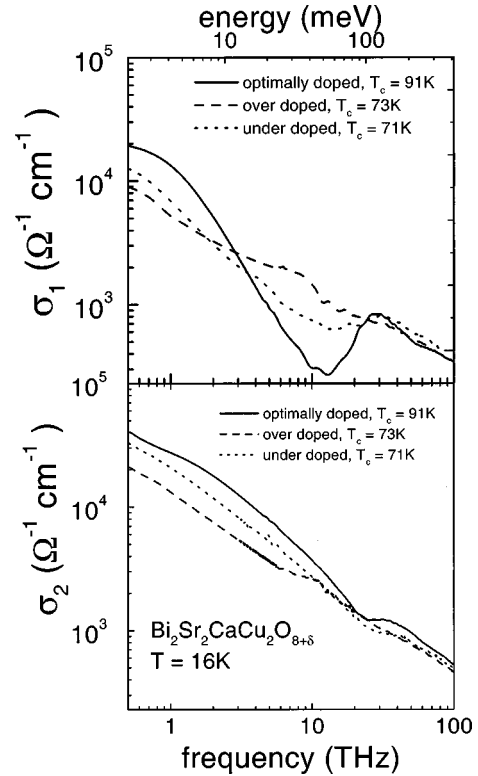


FIG. 4. Real and imaginary parts of the dynamical conductivity at 16 K for under and overdoped crystals compared with an optimally doped crystal.

the magnitude and width of the zero-frequency peak is sensitive to the magnitude of elastic scattering and that an increase will result in pair breaking and a loss of condensate.<sup>4</sup> Through comparison of these calculations with our experimental data it could be interpreted that an increase in elastic scattering produced a broadening in the zero-frequency peak with doping away from optimal. In general, an increase in elastic scattering would be considered to derive from an increase in the impurity concentration. All the crystals investigated were from the same boule and the only compositional changes with doping are changes in the labile oxygen content which is considered to reside in the bismuth oxide layers.<sup>10</sup> An increase in oxygen content systematically increases the hole concentration so that the increase in absorptivity with doping away from optimal is unlikely to increase elastic scattering simply by a change in the labile oxygen content. On the other hand, Mesot *et al.* have recently argued that the gap anisotropy is a function of electronic doping.<sup>11</sup> By comparing photoemission with penetration depth data for  $\text{Bi}_2\text{Sr}_2\text{CaCu}_2\text{O}_{8+\delta}$  they note that the slope of the superfluid density around nodes in the  $d$ -wave order parameter decreases with underdoping. Further, they argue that the gap decreases with overdoping. Both these effects would increase the effectiveness of elastic scatters with doping away from optimal without a change in their population.

Dopant dependent changes in inelastic scattering could also affect the conductivity. For instance, the real part of the conductivity contains information about inelastic scattering processes in the form of the electron-boson spectral density

function  $W(\omega)$ , that can approximately be extracted by an inversion of the conductivity.<sup>12</sup> Recently Carbotte *et al.*<sup>13</sup> have argued that the coupling agent is a spin excitation on the basis of the strong similarity between  $W(\omega)$  and the imaginary part of the spin susceptibility measured by inelastic neutron scattering. Munzar *et al.*<sup>14</sup> have calculated the infrared conductivity of the cuprates and included inelastic scattering of quasiparticles by spin fluctuations described by a spin susceptibility function of the form required to account for the observed neutron scattering results. The calculated conductivity compares well with our data and  $W(\omega)$  extracted from our data displays a shift to lower energies with doping away from optimal (not shown). Thus to explain the observed increase in absorptivity with doping away from optimal requires the spin susceptibility to shift to lower energy. We are not aware of dopant-dependent spin susceptibility data for  $\text{Bi}_2\text{Sr}_2\text{CaCu}_2\text{O}_{8+\delta}$  but for underdoped  $\text{YBa}_2\text{Cu}_3\text{O}_{7-\delta}$  the imaginary part of the spin susceptibility does shift to lower energies with decreasing doping.<sup>15</sup> Thus the observed increase in the absorption when doping away

from optimal may result from dopant dependent changes in inelastic scattering which may in turn be due to changes in the underlying spin excitation spectrum.

We have reported the first measurements of the low frequency absorptivity as a function of doping in  $\text{Bi}_2\text{Sr}_2\text{CaCu}_2\text{O}_{8+\delta}$  to an accuracy that allows the extraction of the frequency-dependent conductivity at 16 K in a spectral region that permits probing of the cross-over between elastic and inelastic scattering. It is observed that there is a rapid change in the nature of this scattering with doping away from optimal. It awaits further experiments to identify the source of the change in scattering that is critical to a full understanding of the low-frequency dynamical response of the cuprates.

The authors acknowledge help from Martin Prenninger and Tony Bittar with spectroscopic measurements, thank Professor K. Kishio and Donald Pooke for supplying and processing crystals, Esther Haines for useful discussions, and the support of the DFG, the DAAD, and New Zealand's FRST.

\*Present address: IBM Deutschland Entwicklung GmbH, Schoenaicher Strasse 220, D-71032 Boeblingen, Germany.

<sup>1</sup>R.G. Buckley, J.L. Tallon, I.W. Brown, M.R. Presland, N.E. Flower, P.W. Gilberd, and M.E. Bowden, *Physica C* **156**, 629 (1988); M.R. Presland, J.L. Tallon, R.G. Buckley, R.S. Liu, and N.E. Flower, *ibid.* **176**, 95 (1991); J.L. Tallon, C. Bernhard, H. Shaked, R. L. Hitterman, and J.D. Jorgensen, *Phys. Rev. B* **51**, 12 911 (1995).

<sup>2</sup>J. Schützmann, B. Gorshunov, K. F. Renk, J. Münzel, A. Zibold, H. P. Geserich, A. Erb, and G. Müller-Vogt, *Phys. Rev. B* **46**, 512 (1992); D. B. Tanner and T. Timusk, in *Physical Properties of High Temperature Superconductors III*, edited by D. M. Ginsberg (World Scientific, Singapore, 1992,) p. 363 and references therein; A. V. Puchkov, D. N. Basov, and T. Timusk, *J. Phys.: Condens. Matter* **8**, 10 049 (1996) and references therein.

<sup>3</sup>K. F. Renk, B. Gorshunov, J. Schützmann, A. Prückl, B. Brunner, J. Betz, S. Orbach, N. Klein, G. Müller, and H. Piel, *Europhys. Lett.* **15**, 661 (1991); D. Miller, P.L. Richards, S. Eternad, A. Inam, T. Venkatesan, B. Dutta, X. D. Wu, C.B. Eom, T.H. Geballe, N. Newman, and B.F. Cole, *Phys. Rev. B* **47**, 8076 (1993); A. Pimenov, A. Loidl, G. Jakob, and H. Adrian, *ibid.* **59**, 4390 (1999); A. Hosseini, R. Harris, Saeid Kamal, P. Dosanjh, J. Preston, Ruixing Liang, W. N Hardy, and D. A. Bonn, *ibid.* **60**, 1349 (1999); J. Corson, J. Orenstein, J.N. Eckstein, and I. Bozovic, *Physica B* **280**, 212 (2000).

<sup>4</sup>J. P. Carbotte, C. Jiang, D. N. Basov, and T. Timusk, *Phys. Rev. B* **51**, 11 798 (1995); M. J. Graf, Mario Palumbo, D. Rainer, and J. A. Sauls, *ibid.* **52**, 10 588 (1995); S. M. Quinlan, P.J. Hirschfeld, and D.J. Scalapino, *ibid.* **53**, 8575 (1996); E.

Schachinger, J.P. Carbotte, and F. Marsiglio, *ibid.* **56**, 2738 (1997).

<sup>5</sup>C. Jiang, E. Schachinger, J.P. Carbotte, D. Basov, and T. Timusk, *Phys. Rev. B* **54**, 1264 (1996).

<sup>6</sup>N. Motohira, K. Kuwahara, T. Hasegawa, K. Kishio, and K. Kitazawa, *J. Ceram. Soc. Jpn.* **97**, 994 (1989).

<sup>7</sup>H. S. Barowski, A. Arnold, M. Prenninger, R.G. Buckley, and K.F. Renk, *J. Low Temp. Phys.* **105**, 785 (1996).

<sup>8</sup>I. Terasaki, S. Tajima, H. Eisaki, H. Takagi, K. Uchinokura, and S. Uchida, *Phys. Rev. B* **41**, 865 (1990).

<sup>9</sup>S.-F. Lee, D.C. Morgan, R.J. Ormeno, D.M. Broun, R.A. Doyle, J.R. Waldram, and K. Kadowaki, *Phys. Rev. Lett.* **77**, 735 (1996).

<sup>10</sup>T. Stoto, D. Pooke, L. Forro, and K. Koshio, *Phys. Rev. B* **54**, 16 147 (1996).

<sup>11</sup>J. Mesot, M.R. Norman, H. Ding, M. Randeria, J.C. Campuzano, A. Paramekanti, H.M. Fretwell, A. Kaminski, T. Takeuchi, T. Yokoya, T. Sato, T. Takahashi, T. Mochiku, and K. Kadowaki, *Phys. Rev. Lett.* **83**, 840 (1999).

<sup>12</sup>F. Marsiglio, T. Startseva, and J.P. Carbotte, *Phys. Lett. A* **245**, 172 (1998).

<sup>13</sup>J. P. Carbotte, E. Schachinger, and D.N. Basov, *Nature (London)* **401**, 354 (1999).

<sup>14</sup>D. Munzar, C. Bernhard, and M. Cardona, *Physica C* **312**, 121 (1999).

<sup>15</sup>P. Bourges, in *The Gap Symmetry and Fluctuations in High Temperature Superconductors*, edited by J. Bok, G. Deutscher, D. Pavuna, and S.A. Wolf (Plenum, New York, 1998).